Available online at www.sciencedirect.com
ScienceDirect
Journal of Power Sources 176 (2008) 410–416
JOURNAL OF POWER SOURCES
www.elsevier.com/locate/jpowsour

Ru oxide supercapacitors with high loadings and high power and energy densities

Xiaorong Liu, Peter G. Pickup *

Department of Chemistry, Memorial University of Newfoundland, St. John's, Newfoundland, Canada A1B 3X7

Received 27 August 2007; accepted 21 October 2007
Available online 30 October 2007

Abstract

Supercapacitors with very high energy and power densities have been constructed with hydrous ruthenium oxide powder prepared by a sol–gel method and annealed at 110 °C. Novel features of the capacitors, which improve their performances, are the use of a carbon fibre paper support, a Nafion separator, and Nafion as a binder. 1 M sulfuric acid was employed as the electrolyte. The performances of the supercapacitors were characterized by cyclic voltammetry, impedance spectroscopy and constant current discharging. The interfacial capacitance increased linearly with increasing ruthenium oxide loading to at least 50 mg cm^{-2} on each electrode. The gravimetric capacitance of the Ru oxide measure by impedance reached 742 F g^{-1} (9.66 F cm^{-2}) at a loading of 13.0 mg cm^{-2}, and an interfacial capacitance of 34.9 F cm^{-2} (682 F g^{-1}) was obtained at 51.2 mg cm^{-2}. The average effective series resistance was 0.55 Ω, the electronic resistance of the electrodes was negligible, and their ionic resistances were <0.42 Ω. The average power density for full discharge at 1 A cm^{-2} for supercapacitors with 10 mg cm^{-2} Ru oxide increased by 39% when 5% Nafion binder was added. The maximum average power density for full discharge was 31.5 W g^{-1} while the maximum energy density was 31.2 Wh kg^{-1}. At a 1 mA discharge rate a specific capacitance of 977 F g^{-1} of Ru oxide was obtained.

Keywords: Supercapacitor; Ru oxide; Ragone plot; Impedance; Power density; Specific capacitance

1. Introduction

Electrochemical capacitors (supercapacitors) are becoming increasingly important as the power demands of portable devices increase and the world moves towards electric vehicles and wider use of renewable energy sources [1–5]. High-surface area carbons [6] are the most widely used capacitive materials, but there is now a rapidly growing effort to develop metal oxide-based systems. These potentially offer higher specific capacitances and higher power densities in aqueous acid or base electrolytes [2,4]. Suitably prepared, amorphous forms of ruthenium oxide have provided the highest specific capacitances reported for any material and are therefore of particular interest for the most demanding applications.

Ruthenium oxide-based supercapacitors were first developed in the late 1970s by Conway in collaboration with Craig of Continental Group Inc. [7]. However, the high cost of Ru has limited them until recently to military applications [4]. Renewed interest in Ru oxide as a supercapacitor material has arisen from improvements in synthesis methods as well as the development of composites aimed at increasing the utilization of Ru [4]. In 1995, Zheng and Jow reported a specific capacitance of 720 F g^{-1} for amorphous Ru oxide prepared by a simple sol–gel process involving mixing of aqueous solutions of NaOH and $RuCl_3$ [8,9]. It was shown that maximum capacitance was obtained by annealing at 150 °C. At higher temperatures, water loss and crystallization leads to a rapid loss of capacitance. This preparation method remains one of the best available, although materials with similar capacitances have been prepared by other routes [10–12].

More recent work has focussed on the development of electrode structures and composites to take best advantage of the high-specific capacitance of hydrous Ru oxide. Jang et al. [13,14] have used electrophoretic deposition with PTFE to enhance the stability of electrode layers, reporting specific

* Corresponding author. Tel.: +1 709 737 8657; fax: +1 709 737 3702.
E-mail address: ppickup@mun.ca (P.G. Pickup).

0378-7753/$ – see front matter © 2007 Elsevier B.V. All rights reserved.
doi:10.1016/j.jpowsour.2007.10.076

energies as high as 17.6 Wh kg^{-1} at 200 W kg^{-1} based on a single electrode. However, they found that the specific capacitance of the Ru oxide dropped with increasing loading on the electrode from 599 F g^{-1} at 0.6 mg cm^{-2} to 350 F g^{-1} at 1.5 mg cm^{-2}. These results were claimed to be similar or superior to others in the literature, although Fang et al. [11] had earlier shown that a specific capacitance of 400 F g^{-1} could be maintained up to a loading of at least 10 mg cm^{-2}. The importance of being able to employ high loadings is that the relative mass of other components of the supercapacitor becomes less significant so that the energy density per gram of device becomes higher. Even at 10 mg cm^{-2} on each electrode, the mass of Ru oxide would only be about 25% of the mass of the device.

In view of these difficulties in maintaining the specific capacitance of Ru oxide at high-electrode loading, there have been numerous studies of Ru oxide composites with various types of carbon. This not only increases the electrode loading that can be employed [15,16], but can also provide higher specific capacitances for the Ru oxide component itself. For example, a specific capacitance of 1170 F g^{-1} has been reported for Ru oxide electrodeposited on carbon nanotubes (1 mg cm^{-2} loading) [17] and 1580 F g^{-1} has been reported for the Ru oxide component (10% by mass) of a physical mixture of Ru oxide and activated carbon [18,19]. However, it should be noted that estimation of these specific capacitances must involve considerable uncertainty due to the small contribution (10%) of the Ru oxide component to the total mass of the composite material. It is also not clear whether such high-specific capacitances can be maintained at high loadings.

In light of the potential benefits of the very high-specific capacitances of hydrous Ru oxides, there have been surprisingly few reports on the performances of supercapacitors employing these materials. Zheng et al. [9] reported an impressive 768 F g^{-1} at 5 mA cm^{-2} for a device with 0.15 g Ru oxide per electrode with no binders. This result was higher than for much lower loadings studied in a conventional cell, and this was attributed the use of PTFE as a binder in the latter experiments. Later, Zheng [15] reported that the maximum power in their device was limited by the ionic resistance of the electrodes. They were able to optimize the power by adding 20% carbon black (Black Pearls 2000) to the electrodes to increase their porosity and electrolyte uptake.

The purpose of the work described here was to further evaluate and optimize the performance of hydrous Ru oxide, prepared following a procedure similar to that described by Zheng and Jow [8], in a supercapacitor. Based on the results of preliminary experiments it was found that outstanding performances (power and energy densities) could be achieved by use of a carbon fibre paper (CFP) support [17], a Nafion membrane separator and an H_2SO_4(aq) electrolyte. Addition of Nafion to the electrodes was also found to be beneficial. The effects of Ru oxide and binder loading have been investigated by cyclic voltammetry, impedance spectroscopy and constant current discharge experiments.

2. Experimental

2.1. Preparation of hydrous ruthenium oxide powder

The hydrous ruthenium oxide power was prepared by a modified version of the sol–gel method described by Zheng et al. [9]. Aqueous 1.5 M Na_2CO_3 was slowly added to a 0.05 M aqueous solution of $RuCl_3{\cdot}xH_2O$ (Precious Metals Online Pty Ltd.) with stirring at room temperature. A ruthenium oxide sol–gel was formed when the pH reached ca. 7, and this was heated to 75 °C. After ca. 5 min, the precipitate completely or partly deposited on the bottom of the container was collected by filtration (Whatman 4) and washed many times with deionized water until the filtrate became cloudy (due to peptization). Finally the Ru oxide sample was dried for a period of 3 h at 110 °C in air.

2.2. Electrode preparation

Ru oxide (2–60 mg) and typically an equal mass of 5% Nafion solution (DuPont) and a few drops of water were ground together to form a paste. This was painted with a brush onto a 1 cm^2 disc (or strip for cyclic voltammetry in a conventional cell) of dried and weighed carbon fibre paper (CFP; Toray^{TM} Carbon Paper, TGP-H-090). The electrodes were dried in air for 10 min at 110 °C, and then re-weighed in order to determine the mass loading of Ru oxide and Nafion binder. Generally, this procedure was repeated a number of times (typically 3) to build-up thick layers and to control the Ru oxide loading. The mass of binder was not included in calculations of specific capacitances, nor power and energy densities.

2.3. Electrochemical characterization

The electrochemical properties of the ruthenium oxide electrodes were initially characterized by cyclic voltammetry using a three-electrode setup (EG&G 273A Potentiostat/Galvanostat) with a Pt wire counter electrode and Ag/AgCl reference electrode. Cyclic voltammetry was also run in two-electrode mode (reference lead connected to the counter electrode) on supercapacitors (sandwich cell; see below). Impedance spectroscopy was conducted on supercapacitors in two-electrode mode by using the EG&G 273A Potentiostat/Galvanostat, a EG&G 5210 lock-in amplifier and EG&G PowerSuite software. The frequency range was from 10 kHz to 5 mHz or 1 mHz, with an amplitude of 10 mV and a dc bias potential of 1 V. The electrolyte was 1 M H_2SO_2(aq) in all cases.

2.4. Supercapacitors

Prototype supercapacitors (two-electrode sandwich cells) were constructed by sandwiching an electrolyte separator (Nafion 115) between two identical 1 cm^2 electrodes consisting of the Ru oxide with a binder spread on carbon fibre paper. Ti plates in polycarbonate blocks were used to make electrical contact, and the whole cell was immersed in 1 M H_2SO_4(aq) containing an Ag/AgCl reference electrode. Air was not excluded from the cell. Cyclic voltammetry and impedance can be

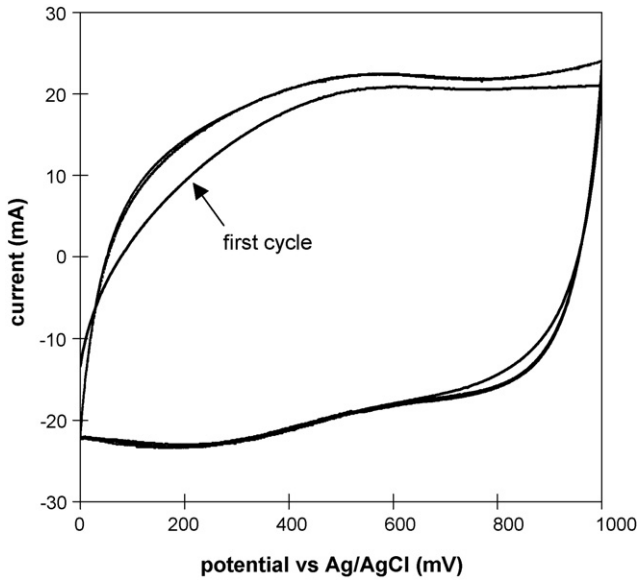

Fig. 1. Cyclic voltammograms (20 mV s^{-1}) of 1.4 mg Ru oxide on CFP in 1 M H_2SO_4(aq). The 1st, 10th, 25th, and 50th scans are shown, but the latter three are virtually indistinguishable.

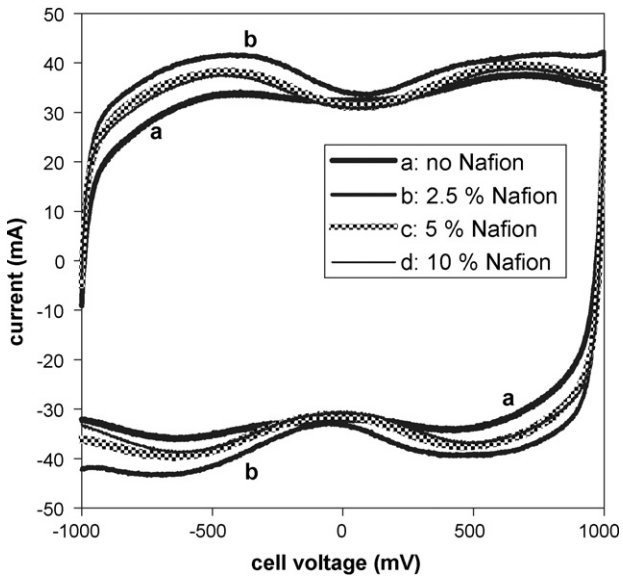

Fig. 2. Cyclic voltammograms (20 mV s^{-1}) of Ru oxide supercapacitors with different amounts of Nafion. Ru oxide loadings were (a) 9.51 mg, (b) 10.35 mg, (c) 10.34 mg, and (d) 10.14 mg.

obtained for each electrode separately (three-electrode mode, with the other electrode acting as the counter electrode), or for the two electrodes simultaneously (i.e. acting as a supercapacitor in two-electrode mode). The sandwich cell allows use of thick layers of capacitive material and minimizes the electrolyte resistance. For constant current discharging experiments, the supercapacitors were charged for a period of 10–70 min at a cell voltage of 1 V.

3. Results

3.1. Cyclic voltammetry in a conventional three-electrode cell

Fig. 1 show cyclic voltammograms in a conventional glass cell for a typical electrode recorded over a period of 50 cycles. Specific capacitances calculated from the average of the anodic and cathodic charge for each cycle are listed in Table 1 together with the ratios of these charges (Q_a/Q_c). After a few cycles, the electrode exhibited stable capacitive behaviour with excellent reversibility ($Q_a/Q_c = 1$). The capacitance was stable at 650 F g^{-1}. Similar results for four other electrodes gave an average specific capacitance of 678 ± 69 F g^{-1}.

Table 1
Anodic to cathodic charge ratios (Q_a/Q_c) and specific capacitances (C_S) from the voltammograms shown in Fig. 1

Scan number	Q_a/Q_c	C_S (F g^{-1})
1	0.89	599
10	1	653
25	1	652
50	1.01	651

3.2. Cyclic voltammetry of supercapacitors

Fig. 2 shows representative cyclic voltammograms for supercapacitors with electrodes prepared with various amounts of Nafion binder, and with a Nafion 115 separator. The Ru oxide loading on each electrode was kept constant at ca. 10 mg. All of the cells showed high-quality capacitive behaviour with excellent reversibility. Addition of 2.5% Nafion binder enhanced the current and capacitance significantly, while higher Nafion loadings, although beneficial, were less effective.

3.3. Constant current discharge

The results of a series of constant current discharge experiments for a supercapacitor with a total of 10 mg cm^{-2} of Ru oxide are shown in Fig. 3. The potential dropped sharply at the beginning of each experiment due to the internal resistance (ESR) and then decreased approximately linearly as expected for a capacitor. ESR values determined from the initial potential drop were typically ca. 0.4 Ω, which is similar to values determined by impedance (see below).

Ragone plots derived from results for cells with different amounts of Nafion binder are shown in Fig. 4, and results for 5% Nafion binder from constant current and cyclic voltammetry experiments are compared in Fig. 5 as log Ragone plots. There is good agreement between the results from the two techniques. The average power for full discharge to 0 V was used for these plots. Maximum powers where typically higher by a factor of ca. 2–3.

It is clear from the results shown in Fig. 4, that the supercapacitors exhibit outstanding performances, and that addition of Nafion to the Ru oxide is very beneficial. For example, the average power density for full discharge at 1 A cm^{-2} increased by 39% when 5% Nafion binder was added. Slightly higher power

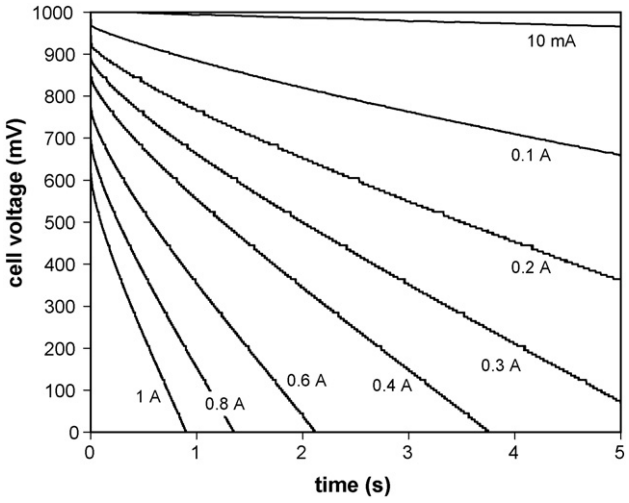

Fig. 3. Constant current discharge plots for a supercapacitor with a total ruthenium oxide loading of 10.34 mg and 5% Nafion binder.

and energy densities were obtained at 10% Nafion, although the difference from the 5% Nafion results is probably not significant. The best average power density for full discharge was 31.5 W g^{-1} while the best energy density was 31.2 Wh kg^{-1}. At a 1 mA discharge rate a specific capacitance of 977 F g^{-1} of Ru oxide was obtained.

3.4. Impedance spectroscopy

Insight into reasons for the outstanding performances of the supercapacitors reported here was obtained from impedance spectroscopy. Fig. 6 shows complex plane impedance (Nyquist) plots for supercapacitors (two-electrode mode) with high-Ru

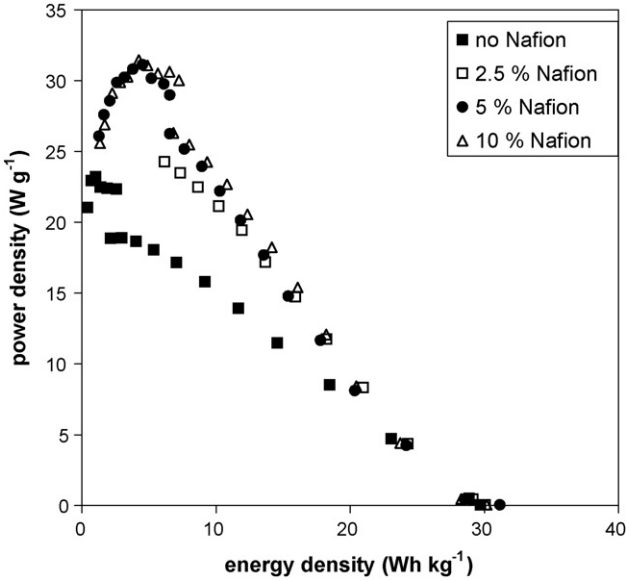

Fig. 4. Ragone plots for supercapacitors with different amounts of Nafion binder. Ruthenium oxide loadings were 9.51, 10.35, 10.34 and 10.14 mg for 0%, 2.5%, 5% and 10% Nafion, respectively. The discontinuities at high powers are due to use of a different potentiostat (Solartron 1286) with lower lead resistances for experiments at currents >1 A.

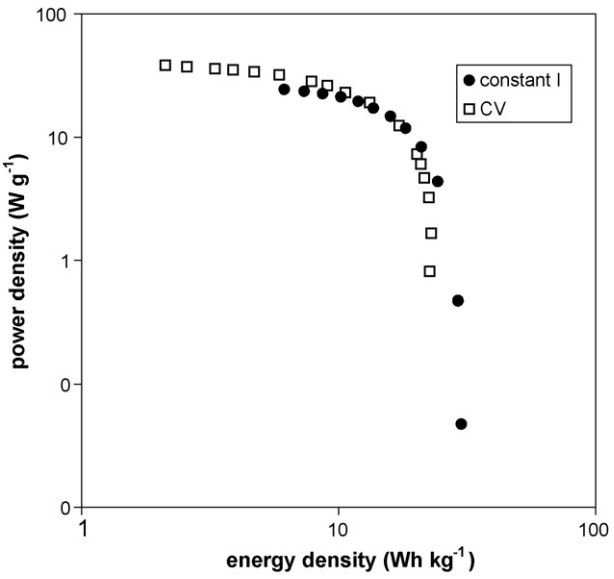

Fig. 5. Ragone plots obtained by different measurement methods. The ruthenium oxide loading was 10.34 mg, with 5% Nafion binder.

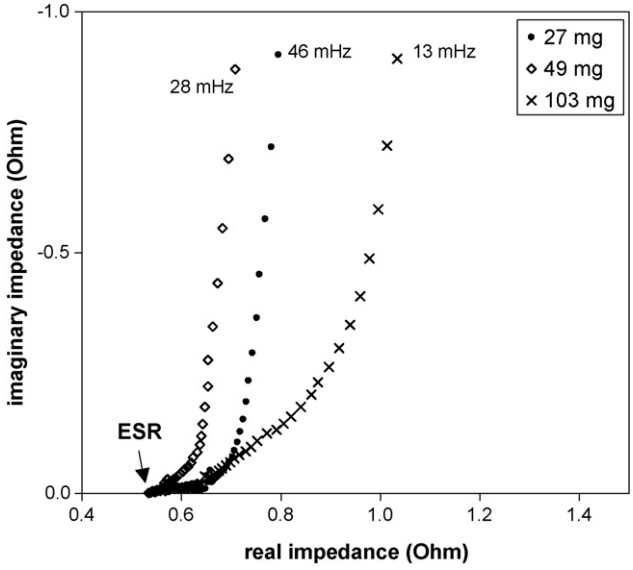

Fig. 6. Complex plane impedance plots for Ru oxide supercapacitors. The total loading of Ru oxide is specified, with 5% Nafion binder.

oxide loadings (the sum of the loading on both electrodes is specified). High-frequency resistances, which correspond to the effective series resistance (ESR) of the supercapacitor, were ca. 0.55 Ω in all cases (Table 2). The ESR includes the membrane resistance (ca. 0.25 Ω), lead, clip and Ti plate resistances, the

Table 2
Effective series resistances (ESR), specific capacitances (C_S) and ionic resistances (R_I) from the impedance data shown in Figs. 6 and 7

Mass of Ru oxide (mg)	ESR (Ω)	R_I (Ω)	C_S (F g^{-1})[a]
27	0.57	0.23	147 (590)
49	0.53	0.25	137 (549)
103	0.55	0.83	139 (555)

[a] Values in parenthesis are single electrode values.

electronic resistances of the Ru oxide and CFP layers, and assorted contact resistances. The lack of a dependence of ESR on the Ru oxide loading shows that the electronic resistances of the Ru oxide layers are insignificant.

The Nyquist plots in Fig. 6 all have the expected shape for porous electrodes [20], consisting of a ca. 45° intermediate region and a ca. 90° low-frequency region. The 27 mg and 103 mg results also show an ill-defined resistance between the ESR and onset of the 45° region that is likely due to a contact resistance. The sum of the ionic resistances of the two capacitive layers (R_I) corresponds to three times the length of the 45° region on the real axis [21]. Values from the data in Fig. 6 are presented in Table 2. It can be seen that R_I increases with the thickness of the Ru oxide layers, as expected. The most notable aspect of these results however is how low the resistances of such high-loading layers are. Clearly, the ionic and electronic resistances of the electrodes play a relatively small role, relative to the separator and contact resistances, in determining the performance of the supercapacitors.

Further insight into the performances of the supercapacitors can be obtained by presentation of the impedance data as "capacitance plots", in which the series capacitance ($C_{series} = -1/\omega Z''$, where ω is the angular frequency and Z'' is the imaginary impedance) is plotted against the real impedance (resistance) [21]. The data in Fig. 6 are plotted in this way in Fig. 7. These plots show that all three devices reach a limiting capacitance by the 5 mHz lowest frequency shown. Specific capacitances for the devices, based on the total Ru oxide loading, are listed in Table 2, together with single electrode values for comparison with data from the three-electrode cell (Fig. 1 and Table 1) and literature results. The single electrode values are four times the device values because the device has double the mass of Ru oxide and its capacitance is half of the capacitance of each electrode, since for two electrodes in series $1/C = 1/C_{electrode\,1} + 1/C_{electrode\,2}$.

The C_S values in Table 2 do not show a significant dependence on loading, indicating full activity of the Ru oxide in

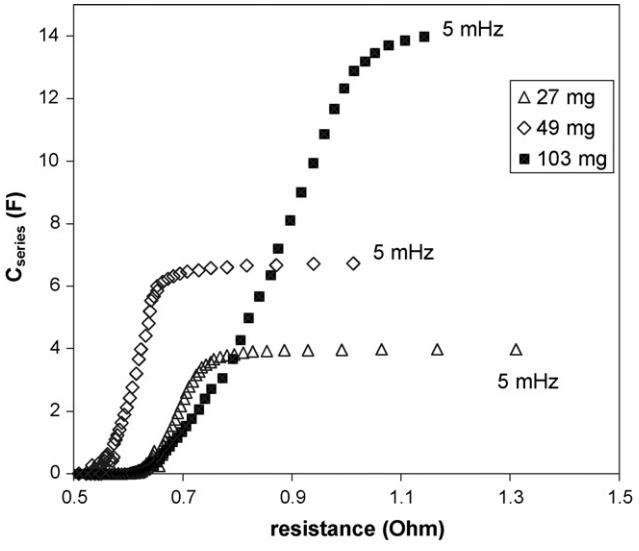

Fig. 7. Capacitance plots derived from the impedance data shown in Fig. 6. The total loading of Ru oxide is specified, with 5% Nafion binder.

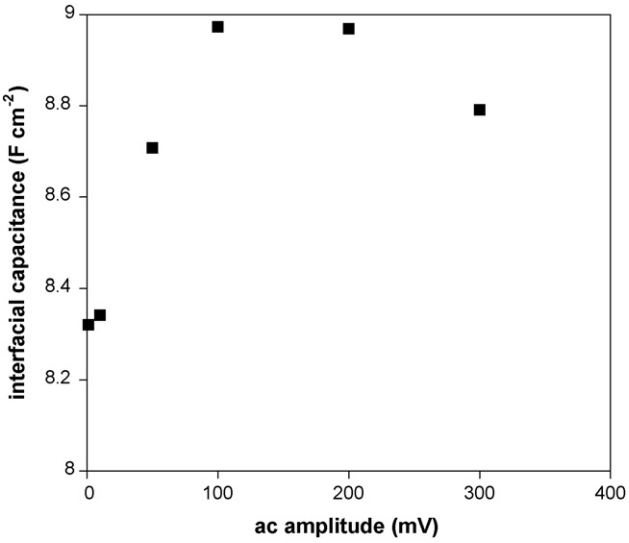

Fig. 8. Limiting capacitance vs. amplitude from impedance experiments on a ruthenium oxide (13.02 mg cm^{-2}) supercapacitor.

each case. The single electrode values are lower than those reported in Table 1 because with the cell charged to 1 V both electrodes have less than optimum capacitance, while the capacitance from cyclic voltammetry is averaged over all potentials and contains some irreversible charge. Irreversible and quasi-reversible processes cause large amplitude measurements (e.g. cyclic voltammetry and constant current discharge) to yield systematically higher capacitances than impedance spectroscopy. This is illustrated in Fig. 8, where the limiting capacitance for a Ru oxide electrode is shown as a function of the ac amplitude used to obtain its impedance. As the amplitude was increased from the normal value of 10 mV, the measured capacitance increased by as much as 7.8%.

The slopes of the intermediate frequency regions of the plots in Fig. 7 are proportional to the ionic conductivities of the Ru oxide layers [21] (these regions correspond to the 45° regions in Fig. 6). It can be seen that the electrodes of the 49 mg device had a significantly better ionic conductivity than for the other two devices. The plot for the 103 mg device shows two different slopes, indicating inhomogeneity in the conductivity of its electrodes [21]. These differences in conductivities between electrodes are presumably a consequence of the manual preparation procedure, which involved spreading of multiple layers of Ru oxide on each electrode to achieve the high loadings used here.

It can also be seen from Fig. 7 that the data for the 27 and 103 mg devices are shifted along the resistance axis relative to the data for 49 mg. This is due in part to their slightly higher ESR values (Table 1), but a larger factor is an ill-defined resistance of ca. 0.1 Ω between the ESR and onset of the 45° region in the impedance plot. There is little capacitance associated with this additional resistance, as can be seen in Fig. 7, and so it is not associated with charging/discharging of the bulk Ru oxide. Since we have seen large interfacial resistances between carbon cloth and the Ti contacts in our cells, we think it most likely that this extra resistance arises at the Ti/CPF interfaces. It is present

to a much smaller extent for the 49 mg device, perhaps due to the presence of less oxide on the Ti surface in this experiment.

The role of the CPF support and Nafion binder used in this work was also explored by impedance spectroscopy, with representative results shown in Fig. 9. Application of the Ru oxide directly to the Ti plates produced supercapacitors with low capacitances and poor performances. From the comparison in Fig. 9 of the impedance of such a supercapacitor with impedances of supercapacitors with the Ru oxide supported on CFP it can be seen that resistances were much higher at all frequencies. It is clear from single electrode impedances (not shown here) that the electrodes with no CFP have large interfacial resistances (presumably at the Ti/Ru oxide interface) and large bulk resistivities (presumably electronic) in the Ru oxide. Further analysis of data for electrodes without CFP was not pursued because of their poor performances.

Addition of Nafion to the Ru oxide electrodes had a relatively minor effect on their impedance, as illustrated in Fig. 9. The main effect was a decrease in the length of the Warburg type (45°) region, indicating improved bulk ionic conductivity, as would be expected from adding a proton conductor. The ESR was also slightly lower, but the difference (<20 mΩ) was too small to be regarded as significant. The impedance did not depend significantly on Nafion loading within the range of 2.5–10% that was investigated.

3.5. Dependence of capacitance on Ru oxide loading

The dependence of the capacitance of individual electrodes on Ru oxide loading was investigated by impedance spectroscopy on supercapacitors with an Ag/AgCl reference electrode in the electrolyte solution (three-electrode mode). All measurements were made at a bias potential of +1.00 V vs. Ag/AgCl. Fig. 10 shows that the interfacial capacitance of the ruthenium oxide electrodes (measured at 5 mHz, or 1 mHz for 50 mg cm^{-2}) increased linearly with increasing ruthenium oxide loading. The specific capacitance of the Ru oxide (also shown in Fig. 10) did not drop significantly as the loading was increased to over 50 mg cm^{-2}. The specific capacitances of ca. 700 F g^{-1} shown in Fig. 10 are higher than the single electrode values reported in Table 2 because the measurements were made at different potentials. The capacitance of the 24.33 mg cm^{-2} electrode was only 541 F g^{-1}, for example, when measured in three-electrode mode at 0.2 V vs. Ag/AgCl.

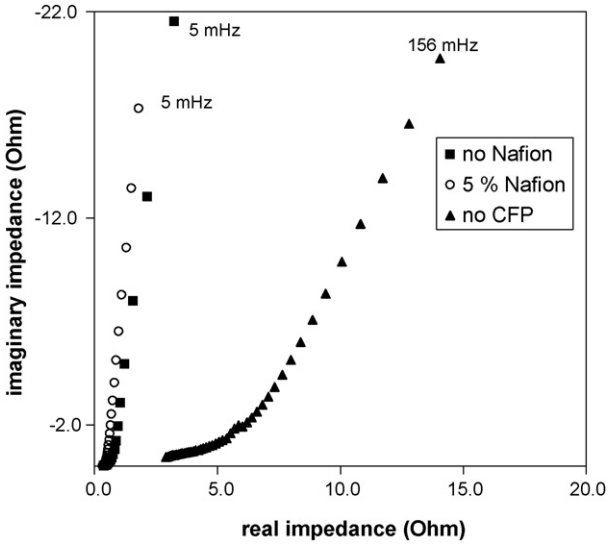

Fig. 9. Complex plane impedance plots for Ru oxide supercapacitors. The total loading of Ru oxide was ca. 10 mg for the two supercapacitors with CFP supports and ca. 5 mg for the supercapacitor with no CPF.

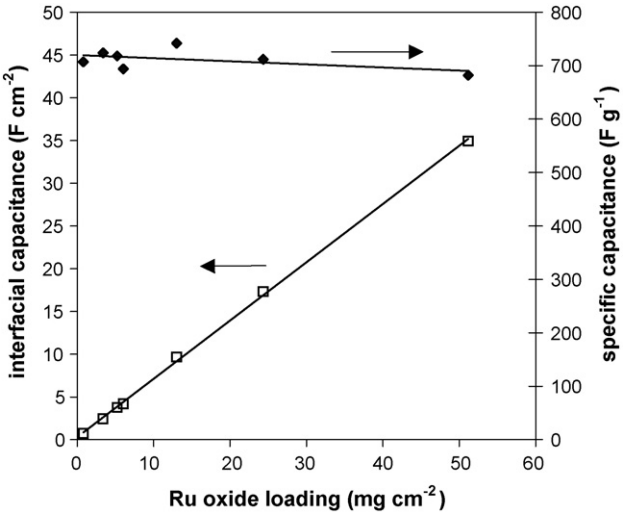

Fig. 10. Interfacial capacitance from impedance at 1 V vs. Ag/AgCl and specific capacitance as a function of hydrous ruthenium oxide loading. 5% Nafion binder was used in all cases.

4. Discussion

The results presented here are remarkable in the high loadings of Ru oxide that have been used without loss of specific capacitance, and the outstanding power densities that have been achieved at high loadings. The following discussion puts these findings into context and explores the reasons for the enhanced performances relative to literature results.

Maintaining a high-specific capacitance at high loadings is crucial to optimizing the energy density of a supercapacitor, since the practical energy density is based on the full mass of the device. Thus for a fixed mass of other components (e.g. ca. 60 mg cm^{-2} for a 0.01 mm thick Al case and 0.01 mm thick separator + electrolyte), the energy density increases appreciably with loading. In theory, it reaches half of its maximum possible value when the mass of active material is equal to the mass of the other components. Reasonably high-active mass loadings are also necessary from a power perspective, because although peak power density decreases with increasing mass of active material (since the peak power is determined only by ESR), high loadings are needed to allow power delivery for a useful period of time.

The dependence of performance on Ru oxide loading is best illustrated by the results shown in Fig. 10. These are similar to results published by Fang et al. [11], although we have obtained much higher interfacial and specific capacitances. They repor-

ted a maximum interfacial capacitance of 4 F cm^{-2} (400 F g^{-1}) obtained with a loading of 10 mg cm^{-2} Ru oxide. We obtained 4.18 F cm^{-2} (694 F g^{-1}) at a 6 mg cm^{-2} loading, and a remarkable 34.9 F cm^{-2} (682 F g^{-1}) at 51.2 mg cm^{-2}. In other studies [13,14], the specific capacitance of Ru oxide similar to ours (i.e. specific capacitance ca. 700 F g^{-1}) was reported to decreased with increasing loading, and this was linked to poor mechanical stability of electrode layers.

Full utilization of the capacitance of the Ru oxide layer requires facile transport of electrons and protons to all of the Ru sites. This can be impeded by electronic and ionic resistances within the oxide layer and at its interfaces with the current collector and electrolyte separator. The impedance results in Figs. 6 and 7 clearly show that these resistances were all low in our electrodes, and this accounts for the fact that high-specific capacitances were maintained even at 50 mg cm^{-2} loadings of Ru oxide per electrode. Our observations point to three key factors that are responsible for these low resistances. First, use of a carbon fibre support minimizes contact resistances between the Ru oxide and Ti plate electrical contact. Secondly, the use of a Nafion binder provides a proton transfer path between particles, so the ruthenium oxide particles located deeper within the layer can participate in the process of proton transfer, thus enhancing the efficiency of charging and discharging. Thirdly, the compression of the layer in the sandwich cell minimizes electronic and contact resistances. The importance of this latter factor is emphasized by Zheng's report of 768 F g^{-1} for a supercpacitor with 0.15 g Ru oxide per electrode [9], albeit with poor power delivery [15].

Our impedance results are considerably simpler than those recently reported by Sugimoto et al. [22] because we have been able to minimize interfacial (charge transfer) resistances. Our interpretation is consequently simpler, although our conclusion that the impedance of the electrodes is dominated by ion (proton) transport is the same. The small residual interfacial resistances that we see may be due to some of the factors that they discuss, such as grain boundaries, electrosorption of ions, and defect/interstitial sites [22].

As generally observed in studies on any electrochemically capacitive material, specific capacitance values vary with the measurement method and timescale employed. Wider measurement amplitudes and longer time-scales yield higher capacitances. It is therefore important to note that none of the capacitances reported in Tables 1 and 2, nor those plotted in Fig. 9 reflect the full capacitance of the Ru oxide that we have used. The key figure, which best represents the full capacitance of the material, is that of 977 F g^{-1} obtained for discharge of a 10 mg cm^{-2} capacitor at 1 mA. This is larger than any other value in the literature for pure Ru oxide.

In addition to maintaining high-specific capacitance at high loadings, the Ragone plots in Figs. 4 and 5 demonstrate that our devices deliver outstanding energy and power densities. The reasons for this are again made clear by the impedance results which show the absence of large resistances that would significantly impair performance. In fact, for the 10 mg cm^{-2} device with the best power density, all resistances attributable to the electrodes were small relative to the ESR. Further work is therefore currently aimed primarily at reduction of the ESR.

5. Conclusions

A specific capacitance of 977 F g^{-1} has been obtained for Ru oxide (5 mg cm^{-2}) in a supercapacitor with 1 M H_2SO_4(aq) electrolyte. Average power densities during full discharge exceed 30 W g^{-1} (peak power >100 W g^{-1}), and energy densities exceed 30 Wh kg^{-1} (108 J g^{-1}).

We believe that these outstanding performances are due primarily to the use of carbon fibre paper as a support for the Ru oxide [17]. This appears to decrease the interfacial resistance between the Ru oxide and the Ti current collector, and stabilize the structure of the Ru oxide layer. The use of Nafion as a binder and a Nafion electrode separator are also beneficial. Impedance results have shown that the ionic resistance of the Ru oxide layer is small, even at high loadings (e.g. ~0.4 Ω at 50 mg).

Acknowledgements

This work was supported by Defence Research and Development Canada, the Natural Sciences and Engineering Council of Canada (NSERC) and Memorial University.

References

[1] B.E. Conway, Electrochemical Supercapacitors, Kluwer, New York, 1999.
[2] R. Kotz, M. Carlen, Electrochim. Acta 45 (2000) 2483.
[3] M. Winter, R.J. Brodd, Chem. Rev. 104 (2004) 4245.
[4] R.A. Huggins, Solid State Ionics 134 (2000) 179.
[5] A.F. Burke, Proc. IEEE 95 (2007) 806.
[6] E. Frackowiak, Phys. Chem. Chem. Phys. 9 (2007) 1774.
[7] B.E. Conway, J. Electrochem. Soc. 138 (1991) 1539.
[8] J.P. Zheng, T.R. Jow, J. Electrochem. Soc. 142 (1995) L6.
[9] J.P. Zheng, P.J. Cygan, T.R. Jow, J. Electrochem. Soc. 142 (1995) 2699.
[10] B.O. Park, C.D. Lokhande, H.S. Park, K.D. Jung, O.S. Joo, J. Power Sources 134 (2004) 148.
[11] Q.L. Fang, D.A. Evans, S.L. Roberson, J.P. Zheng, J. Electrochem. Soc. 148 (2001) A833.
[12] I.H. Kim, K.B. Kim, J. Electrochem. Soc. 153 (2006) A383.
[13] J.H. Jang, A. Kato, K. Machida, K. Naoi, J. Electrochem. Soc. 153 (2006) A321.
[14] J.H. Jang, K. Machida, Y. Kim, K. Naoi, Electrochim. Acta 52 (2006) 1733.
[15] J.P. Zheng, Electrochem. Solid State Lett. 2 (1999) 359.
[16] H. Kim, B.N. Popov, J. Power Sources 104 (2002) 52.
[17] I.H. Kim, J.H. Kim, Y.H. Lee, K.B. Kim, J. Electrochem. Soc. 152 (2005) A2170.
[18] C.C. Hu, W.C. Chen, Electrochim. Acta 49 (2004) 3469.
[19] C.C. Hu, W.C. Chen, K.H. Chang, J. Electrochem. Soc. 151 (2004) A281.
[20] R. De Levie, in: P. Delahay, C.W. Tobias (Eds.), Advances in Electrochemistry and Electrochemical Engineering, vol. 6, Interscience, New York, 1967, pp. 329–397.
[21] M.C. Lefebvre, R.B. Martin, P.G. Pickup, Electrochem. Solid-State Lett. 2 (1999) 259.
[22] W. Sugimoto, H. Iwata, K. Yokoshima, Y. Murakami, Y. Takasu, J. Phys. Chem. B 109 (2005) 7330.